J. Fluid Mech. (2005), *vol.* 527, *pp.* 337–351.
DOI: 10.1017/S0022112004003192 Printed in the United Kingdom

Development of perturbations on a buoyant coastal current

By OLOF H. DAHL

Department of Oceanography, Earth Sciences Centre, Göteborg University,
Box 460, SE-40530 Göteborg, Sweden
olda@oce.gu.se

(Received 1 June 2004 and in revised form 25 October 2004)

The dynamics of small perturbations on a buoyant coastal current is investigated. The system is described using a one and a half-layer model where the active upper layer vanishes at a certain distance from the coast, forming a front. Perturbations are imposed on a steady basic state with no along-coast variation. Analytical solutions are discussed for two special configurations of the basic state: (i) constant along-shore velocity, i.e. a coastal current with triangular cross-section, and (ii) a constant potential vorticity current. Two wave modes are found in both cases: a slowly moving frontally trapped wave, and a coastally trapped wave that moves with approximately the internal Kelvin wave speed plus the speed of the current at the coast. However, these two wave modes are not sufficient to construct a generally shaped initial perturbation. The part of the initial perturbation not covered by the two wave modes will in case (i) split into an infinite number of higher wave modes all travelling faster than the frontal wave and in case (ii) be advected and slowly smeared out by the current. Under the assumption that the current is unidirectional we find that the perturbations always move in the direction of a Kelvin wave, i.e. in the same direction as the coastal current, for all physically relevant cases.

1. Introduction

We investigate the propagation and deformation of a perturbation on a buoyant coastal current. Our aim is to give some insights concerning fluctuations observed in coastal currents.

1.1. *Properties of buoyant coastal currents*

Buoyant coastal currents form when light surface water is accumulated along a coast. Because of the Earth's rotation the light water will not spread over the ocean surface but rather form a current along the coast, with the coast to the right (left) of the current on the northern (southern) hemisphere. A coastal current is typically narrow compared to the size of the ocean basins, with a density front constituting the seaward edge of the current. The buoyant water can be accumulated at the coast by different processes; winds may force buoyant surface water towards the coast, or fresh water supply from rivers may lead to buoyant brackish water along the coast.

Buoyant coastal currents are important for both the basin scale circulation and for local conditions. For instance, along the Swedish west coast much of the brackish water leaving the Baltic is transported by a coastal current into the Skagerrak and the northern North Atlantic (Rodhe 1998). In the northern North Atlantic, the East Greenland Current and the Norwegian Coastal Current are dominating features,

important for the exchange between the Atlantic and the Nordic seas (Hansen & Østerhus 2000).

Variations in the forcing, through changes in the wind field or the river runoff, will change the transport properties of the current. We study the development and propagation of such changes of small amplitude.

1.2. *The problem under consideration: development of perturbations*

The perturbations examined in this study consist of disturbances in the thickness of the surface layer with an amplitude small enough to allow linearization of the equations. We treat the development of the disturbance as an initial-value problem by superposing the perturbations on a stationary basic state. The initial perturbation can have arbitrary shape, provided that the along-current length scale of the perturbations is much greater than the width of the coastal current.

The basic state consists of a homogeneous buoyant upper layer, constituting the coastal current, with a motionless layer of denser water beneath. Some distance away from the coast the upper layer vanishes, forming a density front. The basic state is assumed to be in geostrophic balance, with no variations along the coast. While the along-coast current velocity may vary in the cross-current direction, we require that it does not change sign. The coast is treated as a vertical wall.

To illuminate the evolution of perturbations on these coastal currents we examine two analytically tractable cases. The first case is a coastal current with triangular cross-section, i.e. the upper-layer thickness decreases linearly away from the coast. The second case is a basic state with constant potential vorticity. In the triangular cross-section case, which can be treated as an eigenvalue problem, we obtain an infinite number of wave modes. These modes are absent in the constant potential vorticity case, where instead parts of the perturbation are advected and deformed by the shear flow. However, two wave modes can be found in both cases; a frontally trapped slowly propagating wave and a coastally trapped fast wave.

1.3. *Earlier works*

Many authors have contributed to the theory of coastal currents and coastally trapped waves; Csanady (1982) provides a good overview of coastal phenomena in general. Here follows a brief summary of previous efforts concerning perturbations on coastal currents with bearing on the physical situation examined in the present work.

The stability of coastal currents to long-wave perturbations has been studied in some detail by Killworth & Stern (1982). They showed that coastal currents with close to constant potential vorticity are unstable if the current is not unidirectional. Furthermore, they showed that a more generally shaped coastal current is unstable provided that the following conditions hold at the wall: the alongshore current speed is zero and the potential vorticity is non-zero and increasing towards the wall. Notably, no maximum in the potential vorticity of the flow is needed for these instabilities to occur. In the present work we will only consider stable currents.

Stern (1980) and Paldor (1988) investigated perturbations on coastal currents with zero potential vorticity. Stern studied finite-amplitude perturbations and identified several classes of perturbations, e.g. perturbations that steepen with time or block the transport in the current. Paldor used expansion techniques to study perturbations and found the existence of solitons, governed by the Korteweg–de Vries equation. Both of these studies were restricted to perturbations chosen in such a way that not only the basic state but also the perturbed state had zero potential vorticity. Accordingly, the development from an initial perturbation of arbitrary shape was not considered.

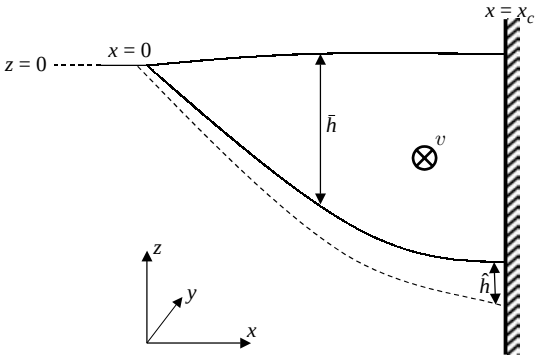

FIGURE 1. A cross-section of the coastal current, where the variables are outlined.

Kubokawa & Hanawa (1984) studied waves on a coastal current with constant but non-zero potential vorticity. They found two wave modes; a Kelvin wavelike 'semigeostrophic coastal wave', and a 'semigeostrophic frontal wave', the latter having its maximum amplitude at the front. The coastal wave propagates downstream faster than the current, while the frontal wave propagates upstream relative to the current velocity. In the present work we find waves similar to these two wave modes as a part of the solution. Kubokawa & Hanawa (1984) also investigated some aspects of the nonlinear development of the two wave modes.

In three of the mentioned papers (Stern 1980; Paldor 1988; Kubokawa & Hanawa 1984), the choice of perturbations was restricted to cases where no perturbation in the potential vorticity occurs. While this restriction simplifies the analysis, it cannot describe a more general case. For example, wind forcing will, in general, cause a perturbation of the potential vorticity field. Here, we study perturbations of arbitrary initial shape.

1.4. *Outline of work*

The paper is organized as follows. In § 2 a model for small perturbations on a coastal current is developed. We show that the problem can be reduced to a single partial differential equation with the perturbation of the upper-layer thickness as dependent variable. In § 3 we present analytical solutions for a current with triangular cross-section, and discuss the nature of the solutions. In § 4 we present analytical solutions for a current with constant potential vorticity, and discuss the properties of the solutions using an illustrative example. Section 5 contains a summary of our results and a brief discussion of the shortcomings of the model. On the basis of the solutions presented in §§ 3 and 4 we discuss the implications of our findings for coastal currents in general.

2. The model

We study small perturbations on a stationary, strictly geostrophic coastal current along a vertical wall, as illustrated in figure 1.

2.1. *Governing equations*

Our model consists of an upper layer with density $\rho - \Delta\rho$ overlying a motionless lower layer with density ρ, on an f-plane. Neglecting friction, observing that the pressure gradient can be written in terms of the upper-layer thickness and assuming

that the pressure gradient in the lower layer is zero, the momentum and continuity equations for the upper layer are:

$$u_t + uu_x + vu_y - fv = -g'h_x, \tag{2.1}$$

$$v_t + uv_x + vv_y + fu = -g'h_y, \tag{2.2}$$

$$h_t + (hu)_x + (hv)_y = 0, \tag{2.3}$$

where $g' = g\Delta\rho/\rho$, f is the Coriolis parameter, h is the thickness of the upper layer, and $\{u,v\}$ are the velocities in the $\{x,y\}$-direction, respectively. A straight coast, parallell to the y-axis, is located at $x = x_c$. The seaward front, where the unperturbed upper layer vanishes, is located at $x = 0$ (cf. figure 1).

Introduce a small perturbation by splitting u, v and h into two parts; a basic state (denoted by bars) and a small perturbation (denoted by circumflexes)

$$u = \bar{u} + \hat{u}, \quad v = \bar{v} + \hat{v}, \quad h = \bar{h} + \hat{h}. \tag{2.4}$$

The basic state constitutes the coastal current, which we demand to be steady, in geostrophic balance and without along-coast variations. Thus,

$$\bar{u} = 0, \quad \bar{h}_y = \bar{v}_y = \bar{h}_t = \bar{v}_t = 0, \quad \bar{v} = \frac{g'}{f}\bar{h}_x, \quad \bar{h}(x = 0) = 0. \tag{2.5}$$

Using this notation in (2.1)–(2.3), and neglecting products of perturbation variables we obtain the following equations for the perturbation (dropping the circumflexes)

$$u_t + \bar{v}u_y - fv = -g'h_x, \tag{2.6}$$

$$v_t + u\bar{v}_x + \bar{v}v_y + fu = -g'h_y, \tag{2.7}$$

$$h_t + (\bar{h}u)_x + \bar{h}v_y + h_y\bar{v} = 0. \tag{2.8}$$

We non-dimensionalize introducing a depth scale H (for instance $H = \bar{h}(x_c)$) and a non-dimensional parameter δ. The same scaling is used by both Killworth & Stern (1982) and Kubokawa & Hanawa (1984). Hence,

$$\{u, v, h\} = \{\delta a u^*, a v^*, H h^*\}, \tag{2.9}$$

$$\{\bar{v}, \bar{h}\} = \{a\bar{v}^*, H\bar{h}^*\}, \tag{2.10}$$

$$\{t, x, y\} = \{f^{-1}\delta^{-1}t^*, f^{-1}ax^*, f^{-1}\delta^{-1}ay^*\}, \tag{2.11}$$

where $a = \sqrt{g'H}$. This scaling implies that the horizontal aspect ratio, i.e. the ratio between the cross- and along-current length scales, is equal to δ. The ratio between the inertial period and the time scale is also equal to δ. Note that we expect $\bar{v}^*$ and $\bar{h}^*$ to be $O(1)$; the perturbation variables u^*,v^* and h^* will on the other hand be $O(\epsilon)$, provided that $\{h, v\} \sim \epsilon\{\bar{h}, \bar{v}\}$.

We assume that

$$\delta \ll 1, \tag{2.12}$$

i.e. the along-current length scale is much longer than the cross-current length scale and the perturbations vary with a time scale much longer than the inertial period. Using the non-dimensional variables we rewrite (2.6)–(2.8) (dropping the asterisks),

$$\delta^2(u_t + \bar{v}u_y) - v = -h_x, \tag{2.13}$$

$$v_t + u\bar{v}_x + \bar{v}v_y + u = -h_y, \tag{2.14}$$

$$h_t + (\bar{h}u)_x + \bar{h}v_y + h_y\bar{v} = 0. \tag{2.15}$$

By combination of (2.13) and (2.14) we obtain expressions for u and v, which can be inserted into (2.15). Neglecting squares of δ, we derive a single equation for the perturbations in terms of h only

$$\left(\frac{\partial}{\partial t}+\bar{v}\frac{\partial}{\partial y}\right)\left(h-\left(\frac{\bar{h}}{1+\bar{v}_x}h_x\right)_x\right)-\left(\frac{\bar{h}}{1+\bar{v}_x}\right)_x h_y=0. \tag{2.16}$$

Returning to dimensional variables we obtain

$$\left(\frac{\partial}{\partial t}+\bar{v}\frac{\partial}{\partial y}\right)\left(h-\frac{g'}{f}\frac{\partial}{\partial x}(\bar{Q}h_x)\right)-g'\bar{Q}_x h_y=0, \tag{2.17}$$

where $\bar{Q}(x)=\bar{h}/(f+\bar{v}_x)$ is the inverse potential vorticity of the basic state.

2.2. *Boundary conditions and the position of the outcropping*

The development of a perturbation is determined from (2.17) together with an initial condition and suitable conditions at the front and the coast. The initial condition is given by the initial shape of the perturbation, i.e. $h(t=0)=h_0(x, y)$. Below we discuss the boundary conditions.

At the coast, the flow through the vertical wall must be zero. Neglecting squares of δ and combining (2.13) and (2.14) gives the following expression for u (in dimensional variables),

$$u=-\frac{g'}{f(f+\bar{v}_x)}(fh_y+h_{xt}+\bar{v}h_{xy}). \tag{2.18}$$

Zero flow through the wall thus implies

$$fh_y+h_{xt}+\bar{v}h_{xy}=0 \qquad \text{at} \qquad x=x_c. \tag{2.19}$$

To illuminate the properties of the frontal boundary we study the outcropping. If we let the outcropping be located at $x=\xi(y, t)$ we can write the dynamic and kinematic boundary conditions

$$h(\xi, y, t)+\bar{h}(\xi)=0, \tag{2.20}$$

$$u(\xi, y, t)=\xi_t+(v(\xi, y, t)+\bar{v}(\xi))\xi_y. \tag{2.21}$$

We make Taylor expansions of these equations around $x=0$ and neglect products of variables associated with the perturbation (i.e. ξ, h, u, v). Eliminating ξ between the equations so obtained, yields

$$h_t+\bar{h}_x u+h_y\bar{v}=0, \tag{2.22}$$

which is exactly (2.8) evaluated at $x=0$. Accordingly (2.20) and (2.21) are automatically satisfied and add no information. To close the problem some other condition is required. In the following two sections, sufficient conditions at the front will come naturally from the requirement that the solutions to (2.13)–(2.15), i.e. h, u and v, stay bounded.

Note that keeping h bounded is also required for the expansion of (2.20) to be valid, and that ξ will be bounded if h is bounded. Furthermore, the expansion of (2.20) gives the position of the outcropping

$$\xi=-\frac{h(0, y, t)}{\bar{h}_x(0)}. \tag{2.23}$$

3. Solutions for a current with triangular cross-section

In this section, we examine perturbations on a basic state where the current speed does not vary across the coastal current, i.e. where $\bar{v}_x \equiv 0$. Thus, the cross-section of the unperturbed upper layer is a triangular wedge;

$$\bar{h} = Ax, \tag{3.1}$$

where A is a constant.

We make the ansatz

$$h = \psi(y - ct)\varphi(x), \tag{3.2}$$

where c is an unknown wave speed, and apply it to (2.17), yielding

$$\bar{Q}(\bar{v} - c)\varphi_{xx} + \bar{Q}_x(\bar{v} - c)\varphi_x + (f\bar{Q}_x - f(\bar{v} - c)/g')\varphi = 0. \tag{3.3}$$

Using the expression for $\bar{h}$, (3.1), we can calculate $\bar{v}$ and $\bar{Q}$ and rewrite (3.3) for a triangular wedge current as

$$Mx\varphi_{xx} + M\varphi_x + c\varphi = 0, \tag{3.4}$$

where

$$M = \frac{g'A}{f^2}\left(\frac{g'A}{f} - c\right) \quad \left[= \frac{\bar{v}}{f}(\bar{v} - c)\right]. \tag{3.5}$$

This equation is a transformation of Bessel's equation and has solutions of the type (Watson 1944, p. 97)

$$\varphi = BJ_0\left(2\sqrt{\frac{cx}{M}}\right) + CY_0\left(2\sqrt{\frac{cx}{M}}\right), \tag{3.6}$$

where B and C are constants, and J_0 and Y_0 are zeroth-order Bessel functions of the first and second kind, respectively.

At the front we require that h, u and v stay bounded. Accordingly, we must set C to zero, since $Y_0 \to -\infty$ as $x \to 0$. This will keep u and v bounded also, and enables us to obtain a unique solution to (3.4) with the help of the boundary condition at the coast (2.19) and an initial state. Application of the ansatz (3.2) to (2.19) yields

$$f\varphi + (\bar{v} - c)\varphi_x = 0. \tag{3.7}$$

By inserting the solution $\varphi = BJ_0(2\sqrt{cx/M})$, we obtain an equation for c

$$fJ_0\left(2\sqrt{\frac{cx_c}{M}}\right) - (\bar{v} - c)\sqrt{\frac{c}{Mx_c}}J_1\left(2\sqrt{\frac{cx_c}{M}}\right) = 0. \tag{3.8}$$

This equation has been solved numerically for c. We discuss the solutions in § 3.2.

3.1. *More general cases*

Using the method of Frobenius we can generalize the treatment of the frontal boundary condition to a whole family of basic states $\bar{h}$. If the basic state has a regular singular point at $x = 0$, we in general find two solutions, corresponding to (3.6), near the front, i.e. one bounded and one unbounded at the front. The calculations are straightforward, but unenlightening.

Observe that (3.3) holds for a general basic state, not only the triangular wedge examined here. Equation (3.3) together with relevant boundary conditions (i.e. (3.7) plus a regularity condition at the front), constitutes an eigenvalue problem with the wave speed c as the eigenvalue. It is important to note that the eigenvalue appears

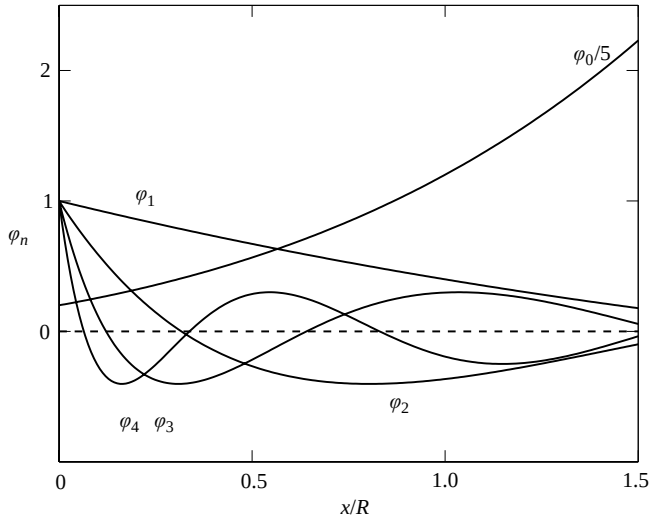

FIGURE 2. The cross-current structure of the first five wave modes, $\varphi_0, \ldots, \varphi_4$, on a coastal current with triangular cross-section. The width of the current, x_c, is set to 1.5 times the Rossby radius, R. Observe that φ_0 has been scaled down by a factor 5.

in the coastal boundary condition (3.7) as well as in (3.3). Thus, we are not dealing with a Sturm–Liouville problem, implying that a complete set of eigenmodes does not necessarily exist.

3.2. *Examination of the solutions*

Let us denote the solutions to (3.8) $c_0, c_1, c_2 \ldots$, with corresponding solutions to (3.4) labelled $\varphi_0, \varphi_1, \varphi_2, \ldots$ where

$$\varphi_n(x) = J_0\left(2\sqrt{\frac{c_n x}{M(c_n)}}\right). \tag{3.9}$$

Inspection of (3.8) indicates that there are an infinite number of possible c if we let $c \to \bar{v}$, owing to the oscillatory nature of Bessel functions. We find only one case where $c > \bar{v}$; we label it c_0 and the corresponding solution φ_0. In all other cases, $0 < c_n < \bar{v}$, and we chose to label the wave speeds such that $c_1 < c_2 < c_3 \ldots$.

We have not been able to prove that the set of eigenmodes $\{\varphi_n\}$ is complete. However, we have used the eigenfunctions to approximate successfully a number of test functions; cosines, exponentials and continuous piecewise linear functions.

Figure 2 shows cross-sections of $\varphi_0, \ldots, \varphi_4$ for a coastal current with a width of 1.5 internal Rossby radii. We note that φ_0 is the only solution that decays away from the coast; all other solutions decay towards the coast, with shorter across-current 'wave-length' as $n \to \infty$. In figure 3, we have plotted the wave speeds of the first four modes as functions of the width of the coastal current. The wave speeds are scaled with the internal Kelvin wave speed

$$c_* = \sqrt{g'\bar{h}(x_c)}. \tag{3.10}$$

We allow the slope A to vary with x_c in order to keep $\bar{h}(x_c)$ constant. In the limit of an infinitely wide current (i.e. $x_c \to \infty$), c_0 is equal to c_*, while $c_n = 0$ for $n > 1$. When the width of the current is finite, c_0 is somewhat smaller than the sum of the current speed $\bar{v}$ and the speed of an internal Kelvin wave c_* while c_1 is significantly slower

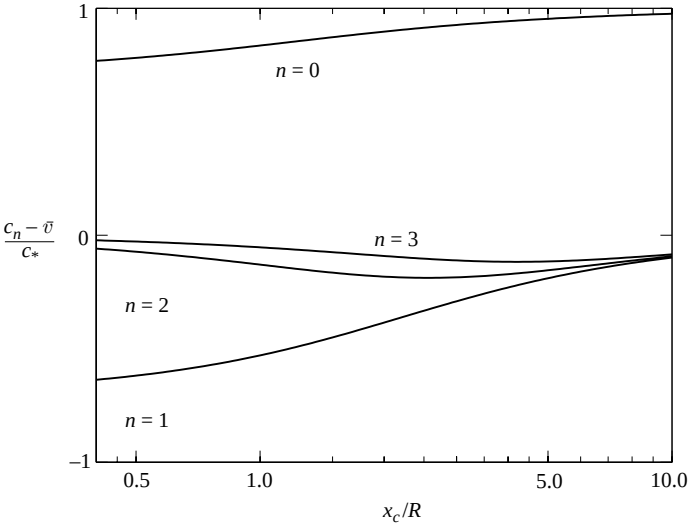

FIGURE 3. The curves show the wave speed minus the current speed, normalized with the Kelvin wave speed, as a function of the width of the coastal current. Each curve corresponds to a different wave mode φ_n on a triangular cross-section current.

than the current speed. For larger values of n, the wave speed quickly approaches the speed of the current, i.e. the higher-order wave modes are more or less advected by the current.

4. Solutions for a constant potential vorticity current

In simple models of fronts and coastal currents it is often assumed that the current has constant potential vorticity (Kubokawa & Hanawa 1984; Killworth & Stern 1982, § 3). This assumption can be justified by requiring that the current originates from a body of water with homogenous potential vorticity. Since potential vorticity is conserved for fluid particles in the absence of diapycnal mixing and friction, the potential vorticity will then stay constant (Pedlosky 1987).

In this section we will study perturbations on a basic state with constant potential vorticity. For convenience, we have used the inverse potential vorticity as a parameter rather than the potential vorticity itself. The basic-state upper-layer thickness $\bar{h}$, can be derived from the requirement that the inverse potential vorticity $\bar{Q} = \bar{h}/(f + \bar{v}_x)$ is constant. Since we do not allow any along-current variations and demand that $\bar{h}$ vanishes at $x = 0$, the thickness of the unperturbed upper layer will be given by

$$\bar{h} = f\bar{Q} + A_1 \mathrm{e}^{-x/R_D} + A_2 \mathrm{e}^{x/R_D}, \tag{4.1}$$

where

$$A_1 + A_2 = -f\bar{Q}, \tag{4.2}$$

and

$$R_D = \sqrt{\frac{g'\bar{Q}}{f}}. \tag{4.3}$$

This case has three degrees of freedom; we can choose e.g. $\bar{Q}$, x_c and A_1 independently. In this study, we limit these parameters to cases where $\bar{h}$ is growing monotonically towards the coast, implying that the along-current velocity $\bar{v}$ is always positive.

The eigenvalue approach used in § 3 cannot be used here. Since $\bar{Q}_x = 0$, the last term on the left-hand side of (3.3) disappears. We can thus remove the eigenvalue by dividing all terms by $\bar{v} - c$. The resulting expression cannot describe an arbitrary initial perturbation; instead we have to derive our solutions directly from (2.17).

Now, since $\bar{Q}_x = 0$, (2.17) reduces to

$$\left(\frac{\partial}{\partial t} + \bar{v}\frac{\partial}{\partial y}\right)\left(h - R_D^2 h_{xx}\right) = 0, \tag{4.4}$$

which implies that

$$h_{xx} - \frac{1}{R_D^2}h = \Psi(x, \bar{v}(x)t - y), \tag{4.5}$$

where Ψ is given by the initial distribution of h

$$\Psi(x, -y) = \left(h_{xx} - \frac{1}{R_D^2}h\right)\Big|_{t=0}. \tag{4.6}$$

Note that the perturbation of the inverse potential vorticity may be written as

$$\left(h - R_D^2 h_{xx}\right)/(f + \bar{v}_x) \tag{4.7}$$

and that (4.4) thus states that potential vorticity is conserved for fluid particles.

Equation (4.5) can be solved using the method of variation of parameters, yielding (Bender & Orszag 1978, p. 15):

$$h = C(y,t)\mathrm{e}^{-x/R_D} + D(y,t)\mathrm{e}^{x/R_D} + R_D\int_0^x \Psi(\xi, \bar{v}(\xi)t - y)\sinh\left(\frac{x-\xi}{R_D}\right)\mathrm{d}\xi. \tag{4.8}$$

Let us now examine the front. In (4.8), $\bar{h}$ and $\bar{v}$ stay bounded as $x \to 0$. As a consequence the approach from § 3 does not work here. However, we can obtain a boundary condition for the front from (2.18) by noting that $f + \bar{v}_x \to 0$ as $x \to 0$. Accordingly, $|u| \to \infty$ unless we require

$$f h_y + h_{xt} + \bar{v}h_{xy} = 0 \qquad \text{at} \qquad x = 0. \tag{4.9}$$

Using this as the frontal boundary condition we can close the problem. Note the similarity between (4.9) and the coastal boundary condition (2.19).

4.1. *The special case* $\Psi = 0$

Let us first consider the case where the potential vorticity of the perturbed state is the same as for the basic state, i.e.

$$\Psi = 0. \tag{4.10}$$

Setting $\Psi = 0$ implies that the integral term of (4.8) vanishes. Thus, the initial distribution of the perturbation must be of the form

$$h = G_1(y)\mathrm{e}^{-x/R_D} + G_2(y)\mathrm{e}^{x/R_D} \qquad \text{at} \qquad t = 0, \tag{4.11}$$

where G_1 and G_2 are arbitrary functions.

Using the boundary conditions, (2.19) and (4.9), we find two wave modes h_0 and h_1 of the form

$$h_i = B_i(c_i t - y)\left(\mathrm{e}^{-x/R_D} + \phi_i \mathrm{e}^{x/R_D}\right) \qquad (i = 0, 1), \tag{4.12}$$

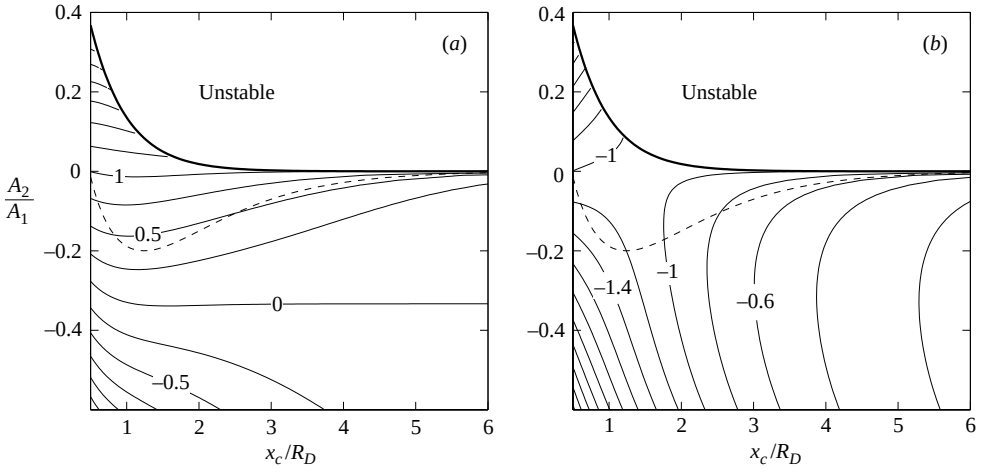

FIGURE 4. The propagation speeds of waves on a constant potential vorticity current: (*a*) isolines of $(c_0-\bar{v}(x_c))/c_*$, (*b*) isolines of $(c_1-\bar{v}(0))/c_*$. The structure of the current is given by A_2/A_1 and the width of the current x_c/R_D. Below the dashed line $\bar{v}(x_c) > c_*$ and above the thick line the current would go backwards at the coast, i.e. it would be unstable (Killworth & Stern 1982). Thus, the most physically realistic cases are found between the dashed and the thick lines.

where the wave speeds c_i and the constants ϕ_i are given by the boundary conditions. B_i are determined from the initial condition, (4.11). The sum of h_0 and h_1 can satisfy any initial condition for which $\Psi = 0$.

The two wave modes have different properties. One mode, here labelled h_0, has its largest amplitude at the coast and travels downstream faster than the maximum speed in the current. The other mode, h_1, has its largest amplitude at the front and travels slower than the minimum speed of the current. The two wave modes closely resemble the modes φ_0 and φ_1 from the triangular cross-section case.

Figure 4 show isolines of the wave velocities c_0 and c_1 minus the current speed at the coast and the front, respectively, scaled with the internal Kelvin wave speed, c_*. To show the variation with different configurations of the background current we have plotted the isolines in the space spanned by the quotient A_2/A_1 and the non-dimensional width, x_c/R_D, of the coastal current.

The ratio A_2/A_1 is small in most geophysical applications since the variation of $\bar{h}$ tends to be largest close to the front (cf. 4.1). If $A_2/A_1 > 0$ (the upper part of the diagrams) the flow is stable only if A_2/A_1 is sufficiently small (Killworth & Stern 1982). If $A_2/A_1 < 0$ (the lower part of the diagrams), the along-coast current speed becomes large close to the coast for wide currents. Increasingly negative A_2/A_1 implies that the Richardson number at the coast grows unrealistically large. In figure 4 we have plotted the curve $\bar{v}(x_c) = c_*$ (the dashed line), corresponding to a Richardson number equal to one, with the Richardson number defined as

$$R_i = \frac{c_*^2}{\bar{v}(x_c)^2}. \tag{4.13}$$

In general, c_1 is positive and close to zero for most realistic coastal currents. For practical purposes, such as comparison with measurements, the wave speeds can be approximated as

$$c_0 \approx \bar{v}(x_c) + c_*, \tag{4.14}$$

$$c_1 \approx \bar{v}(0) - c_*. \tag{4.15}$$

This approximation becomes more accurate when $|A_2/A_1|$ is small. If $A_2 = 0$, and thus

$$\bar{h} = f\bar{Q}\left(1 - \mathrm{e}^{-x/R_D}\right), \tag{4.16}$$

the error is smaller than $0.06\,c_*$ for all choices of x_c/R_D. If the current is infinitely wide and $A_2 = 0$ the approximation becomes exact. In that case the front and the coast will both be equivalent to a wall where the depth of the upper layer is equal to $f\bar{Q}$. This gives waves with the same properties as ordinary internal Kelvin waves advected by the current speed at the respective boundary.

Both Killworth & Stern (1982) and Kubokawa & Hanawa (1984) derive waves similar to the two wave modes found here. Killworth & Stern (1982) focus on instabilities and do not describe the waves in any detail. Kubokawa & Hanawa (1984) find a 'semigeostrophic coastal wave', corresponding to the h_0 mode (4.12), and a 'semigeostrophic frontal wave', corresponding to h_1. However, these waves cannot satisfy an arbitrarily chosen initial perturbation, and we extend our analysis to cover an arbitrary initial perturbation in the next section.

4.2. *The case* $\Psi \neq 0$

Knowing the solutions (4.12) to the case with $\Psi = 0$, we rewrite the solution to the general case (4.8)

$$h = C_0(y,t)\left(\mathrm{e}^{-x/R_D} + \phi_0\mathrm{e}^{x/R_D}\right) + C_1(y,t)\left(\mathrm{e}^{-x/R_D} + \phi_1\mathrm{e}^{x/R_D}\right) + R_D\int_0^x \Psi(\xi, \bar{v}(\xi)t - y)\sinh\left(\frac{x-\xi}{R_D}\right)\mathrm{d}\xi, \tag{4.17}$$

where C_0 and C_1 are unknown functions of y and t. Applying the boundary conditions (2.19) and (4.9) we can, after tedious algebra, show that C_0 and C_1 are given by

$$\begin{aligned} C_i = {} & B_i(c_i t - y) \\ & + \frac{2R_D\left(1 - \phi_i\mathrm{e}^{2x_c/R_D}\right)}{\left(\phi_i^2\mathrm{e}^{2x_c/R_D} - 1\right)\cosh(x_c/R_D)}\int_0^t\int_0^{x_c} \Psi_2(\xi, (\bar{v}(\xi) - c_i)\tau + c_i t - y) \\ & \times\left[(\bar{v}(\xi) - \bar{v}(x_c))\cosh\left(\frac{x_c - \xi}{R_D}\right) - R_D f\sinh\left(\frac{x_c - \xi}{R_D}\right)\right]\mathrm{d}\xi\,\mathrm{d}\tau \quad \text{for } i = 0, 1, \end{aligned} \tag{4.18}$$

where

$$\Psi_2(x,\eta) = \frac{\partial}{\partial\eta}\Psi(x,\eta) \tag{4.19}$$

and B_0 and B_1 are functions of a $(c_i t - y)$ only. B_0, B_1 and Ψ are determined from the initial condition, with Ψ defined by (4.6).

In figure 5(*a–c*) we show an example of the development from an initial perturbation given by

$$h(x,y) = A\mathrm{e}^{-(y/L_p)^2}, \quad 0 \leqslant x \leqslant x_c, \tag{4.20}$$

where $L_p = 7R_D$ sets the length scale of the perturbation and A the amplitude. The basic current structure is given by (4.16), with $x_c = 2R_D$, and is illustrated in figure 5(*d*). With the help of (4.17) and (4.18) we can interpret figure 5 and give some predictions of the development of an initial perturbation with limited along-coast extension in general. The shear, represented by $\bar{v}(\xi)$ under the integral sign, will slowly smear out the contribution to h from the third term on the right-hand side of (4.17). In the long time limit the integral tends to zero in every point, leaving us with the wave

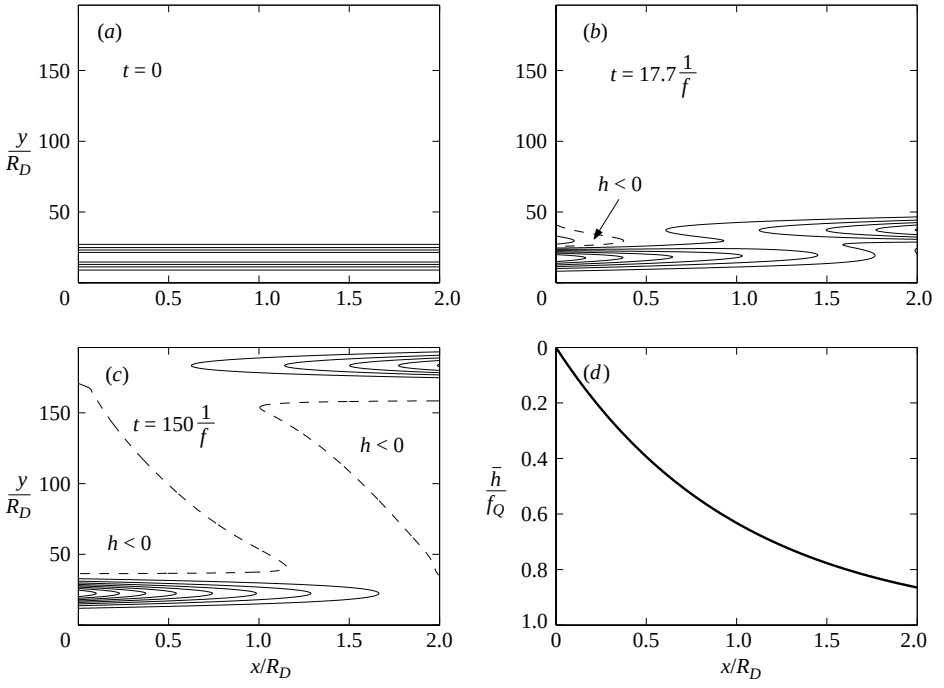

FIGURE 5. (a–c) show snapshots from the development of an initial disturbance given by (4.20), with $L_p = 7\,R_D$, on a constant potential vorticity current, seen from above. The isolines are equidistant in h, with the dashed one representing $h = 0$. Note that the amplitude of the frontal wave mode (cf. (c)) is much larger than the amplitude of the initial disturbance (cf. (a)). (d) shows the depth of the background current.

solutions, h_0 and h_1, discussed in § 4.1. Thus, an observer will, in the long time limit, only see a coastal and a frontal wave. In figure 5(c) we can see how the two waves have separated. The integral term in (4.17) is reduced in amplitude, as it is smeared out over the whole area between the two waves.

Note that the three terms on the right-hand side of (4.17) cannot be interpreted as three independent wave modes; the integral (the third term) contains contributions to the coastal as well as the frontal wave mode. This leads to an apparent growth or decline of the amplitude of the coastal and frontal waves, as exemplified by figure 5(a–c); the frontal wave in figure 5(c) has about twice the amplitude of the initial perturbation in figure 5(a). For large t, when the waves and the integral term in (4.17) have separated, C_0 and C_1 become functions of $(c_i t - y)$ only, and (4.18) gives the amplitudes of the coastal and frontal wave modes.

5. Concluding remarks

5.1. *Summary*

This study outlines the development of a small initial perturbation on a buoyant coastal current along a vertical wall, overlying a motionless deep layer. The basic state is stationary and without variations along the coast. Under the assumption that the perturbations are long compared to the width of the current, we derive an equation for the development of the perturbation (2.17). Making a wave ansatz (3.2), we find that the possible basic states can be divided into two mathematically different

categories. (i) Except for certain special cases application of the ansatz leads to an eigenvalue problem with the wave speed c as the eigenvalue, as detailed in § 3. (ii) If the basic state has constant potential vorticity the eigenvalue disappears from the governing equation (2.17), but remains in the boundary conditions. Solution of the degenerate eigenvalue problem leads to the two wave solutions presented in § 4.1. The full solution for a basic state with constant potential vorticity cannot be obtained by making a wave ansatz, as detailed in § 4.

We solve the problem analytically for two special cases, one in each category. In the first case, which belongs to category (i), we have chosen a basic state with constant current speed, implying that the upper layer has a triangular cross-section. We obtain an infinite number of wave mode solutions to the eigenvalue problem. All modes except one have their maximum amplitude at the front and move slower than the current speed. The first and fastest mode, φ_0, has its maximum amplitude at the coast and moves almost with the speed of an internal Kelvin wave plus the current speed. The second mode, φ_1, is the slowest; it is almost stationary, moving slowly in the same direction as the current. High-order modes are almost advected by the current, moving only very slowly relative to the basic current.

In the second case we investigate a basic state where the upper layer has constant potential vorticity. We find two wave modes similar to the fastest and slowest mode of the triangular cross-section case. The complete solution to the constant potential vorticity case also includes a non-wavelike part which is advected and deformed by the current.

Despite the fact that the mathematical properties of the two cases are different, the solutions show pronounced similarities. In both cases, the solution can be divided into three parts: a frontal wave mode; a coastal wave mode; and a part that moves more or less with the current. This result suggests that perturbations on a more general basic state probably evolve in much the same way as in the two investigated cases.

5.2. *Consequences of arbitrary initial perturbations*

In the present work, unlike earlier works, we consider the development of arbitrary initial perturbations. We have noted two features that deserve special attention. (i) Parts of the perturbation will essentially be advected by the current. (ii) The amplitude of the coastal and frontal waves may deviate significantly from the amplitude of the initial perturbation, owing to the superposition of wave modes. This phenomenon is illustrated in figure 5(a–c), where the amplitude of the frontal wave mode is more than twice as large as the amplitude of the initial perturbation.

5.3. *Waves on triangular cross-section currents*

Wave perturbations on a basic state with triangular cross-section attached to a coast, have to our knowledge not been analysed previously. However, Cushman-Roisin (1986) derived solutions for an arbitrary small initial perturbation on a triangular cross-section current far from a wall. The solutions contain a set of wave modes that have similar cross-current structure to those found here, but different dispersion properties. The scaling assumptions used by Cushman-Roisin also deviate from our assumptions. Here, we assume that the cross-current length scale is of order R, the internal Rossby radius, while Cushman-Roisin assumes that all length scales are much larger than R.

5.4. *Perturbations as meanders*

Perturbations on natural currents often develop into meanders and eddies on the front, see for example Johannessen *et al.* (1989). As can be seen from (2.23) the displacement of the outcropping is proportional to the amplitude of the perturbation

at $x = 0$. Since the frontal wave modes have their maximum amplitude at the front, meanders will mainly be described by these modes. Thus, stationary meanders would essentially be manifestations of the first frontal wave mode, whereas moving meanders correspond to the higher-order modes. The interaction between topography and the first frontal wave mode is of special interest. If a topographic feature excites the almost stationary first frontal wave mode we expect a growing meander. Since the topography may continuously supply energy to the wave, even a relatively small topographic feature could lead to a large stationary meander.

5.5. *Limitations of the model*

Our analysis has some obvious limitations. Most importantly, the presence of a sloping topography will necessarily lead to motions in the lower layer, breaking one of the main assumptions of the analysis. A sloping coast, in contrast to a vertical wall, will also allow topographic wave modes, cf. Csanady (1982).

We expect that an active lower layer leads to changes in the propagation speed of the waves and possibly to instability. Killworth, Paldor & Stern (1984) examined a free front far away from a wall, overlying an active lower layer with no motion in the basic state. They showed that the front is always unstable to long waves. When the thickness of the lower layer was decreased the growth rate and propagation speed of the waves increased. Kubokawa (1988) and Paldor & Ghil (1991) studied instabilities on a coastal current with zero potential vorticity overlying an active lower layer, but also found linearly stable regimes when the lower layer was deep enough.

Friction, both against the wall and through mixing at the front, is not included in the model. The presence of friction would not only affect the perturbations, but also the basic state; a consistent basic state would either be non-stationary or changing along the coast. We also expect the perturbations to become damped.

Furthermore, we have not taken critical layers into account, i.e. areas around points where the wave and current speed are equal ($\bar{v}(x) = c$). The presence of critical layers will complicate the analysis; either turbulence or nonlinear effects will be important there. The triangular wedge case has no critical layers, while the constant potential vorticity case has two regimes where critical layers can occur. In a current with a flow reversal, the presence of a critical layer leads to instabilities as proved by Killworth & Stern (1982) (the area marked 'Unstable' in figure 4). The other regime where constant potential vorticity currents have a critical layer is characterized by unrealistically high current speeds at the coast. (The area below the curve $(c_0 - v(x_c))/c_* = 0$ in figure 4*a*). Finally, it should be noted that basic states with zero potential vorticity as used by Stern (1980) and Paldor (1988) are not included in the present analysis.

Financial support for this work was provided by the Faculty of Science, Göteborg University. The author is grateful to his supervisors G. Walin and G. Broström for their useful advice. The author also thanks D. Sahni and G. Rosenblioum for helpful discussions and an anonymous reviewer for the clarifying comments on frontal boundary conditions.

REFERENCES

Bender, C. M. & Orszag, S. A. 1978 *Advanced Mathematical Methods for Scientists and Engineers: Asymptotic Methods and Perturbation Theory*. McGraw-Hill.

Csanady, G. T. 1982 *Circulation in the Coastal Ocean*. D. Reidel.

Cushman-Roisin, B. 1986 Frontal geostrophic dynamics. *J. Phys. Oceanogr.* **16**, 132–143.

Hansen, B. & Østerhus, S. 2000 North Atlantic–Nordic Seas exchanges. *Prog. Oceanogr.* **45**, 109–208.

Johannessen, J. A., Svendsen, E., Sandven, S., Johannessen, O. M. & Lygre, K. 1989 Three-dimensional structure of mesoscale eddies in the norwegian coastal current. *J. Phys. Oceanogr.* **19**, 3–19.

Killworth, P. D., Paldor, N. & Stern, M. E. 1984 Wave propagation and growth on a surface front in a two-layer geostrophic current. *J. Mar. Res.* **42**, 761–785.

Killworth, P. D. & Stern, M. E. 1982 Instabilities on density-driven boundary currents and fronts. *Geophys. Astrophys. Fluid Dyn.* **22**, 1–28.

Kubokawa, A. 1988 Instability and nonlinear evolution of a density-driven coastal current with a surface front in a two-layer ocean. *Geophys. Astrophys. Fluid Dyn.* **40**, 195–223.

Kubokawa, A. & Hanawa, K. 1984 A theory of semigeostrophic gravity waves and its applications to the intrusion of a density current along a coast. Part 1. Semigeostrophic gravity waves. *J. Oceanogr. Soc. Japan* **40**, 247–259.

Paldor, N. 1988 Amplitude-wavelength relations of non-linear frontal waves on coastal currents. *J. Phys. Oceanogr.* **18**, 753–760.

Paldor, N. & Ghil, M. 1991 Shortwave instabilities of coastal currents. *Geophys. Astrophys. Fluid Dyn.* **58**, 225–241.

Pedlosky, J. 1987 *Geophysical Fluid Dynamics*, 2nd edn. Springer.

Rodhe, J. 1998 The Baltic and North Seas: a process oriented review of the physical oceanography. In *The Sea* (ed. A. R. Robinson & K. H. Brink), vol. 11, pp. 699–732. J. Wiley.

Stern, M. E. 1980 Geostrophic fronts, bores, breaking and blocking waves. *J. Fluid Mech.* **99**, 687–703.

Watson, G. N. 1944 *A Treatise on the Theory of Bessel Functions*, 2nd edn. Cambridge University Press.